Sains Malaysiana 53(10)(2024): 3511-3520
http://doi.org/10.17576/jsm-2024-5310-23

Enhancing Indoor Photovoltaic Performance of Inverted Type Organic Solar Cell by Controlling Photoactive Layer Solution Concentration

(Meningkatkan Prestasi Fotovoltaik Dalaman Sel Suria Organik Jenis Terbalik dengan Mengawal Kepekatan Larutan Lapisan Fotoaktif)

MOHAMED NAFEER WAJIDH[1], NOUR ATTALLAH ISSA[1], KAM SHENG LAU[1], SIN TEE TAN[2], CHIN HUA CHIA[1], MUSLIZAINUN MUSTAPHA[1], MOHAMMAD HAFIZUDDIN HJ JUMALI[1] & CHI CHIN YAP[1,*]

[1]*Department of Applied Physics, Faculty of Science and Technology, Universiti Kebangsaan Malaysia, 43600 UKM Bangi, Selangor, Malaysia*
[2]*Department of Physics, Faculty of Science, Universiti Putra Malaysia, 43400 UPM Serdang, Selangor, Malaysia*

Received: 1 April 2024/Accepted: 27 August 2024

ABSTRACT

With the development of various low-power indoor electronic devices, indoor photovoltaics, particularly organic solar cells (OSCs) have attracted a lot of interest in recent years. Increasing the light absorption and suppressing the leakage current are pivotal to improve the indoor photovoltaic performance of OSCs. In this study, the carbon quantum dots (CQDs)-incorporated photoactive layer solution concentration was varied to improve the photovoltaic performance under 1-sun and indoor white LED illumination. The photoactive layer was composed of (6,6)-phenyl-C61-butyric acid methyl ester) (PCBM) as the acceptor and poly(3-hexylthiophene) (P3HT) as the donor. The ZnO electron transport layer was deposited on fluorine-doped tin oxide (FTO)-coated glass substrates using a spin coating technique. The photoactive layers with different solution concentrations were spin coated on top of the ZnO layer. For device completion, silver anode was thermally evaporated. It is interesting to find that the optimum solution concentration obtained under white LED illumination is larger than that under 1-sun illumination. The maximum power conversion efficiency (PCE).of 0.95% was obtained under 1-sun illumination for device with the solution concentration of 36 mg/mL, whereas, under white LED illumination, the highest PCE of 3.59% was obtained for the device with solution concentration of 48 mg/mL. The discrepancy is ascribed to the higher light absorption of thicker photoactive layer and less significant charge recombination loss under weak light intensity. This study highlights the importance of using different optimization strategies to improve the photovoltaic performance of OSCs for outdoor and indoor applications.
Keywords: Carbon quantum dots; charge recombination; leakage current; light absorption; thickness

ABSTRAK

Dengan pembangunan pelbagai peranti elektronik dalaman berkuasa rendah, fotovoltaik dalaman, terutamanya sel suria organik (OSC) telah menarik banyak perhatian sejak beberapa tahun kebelakangan ini. Peningkatan penyerapan cahaya dan pengurangan kebocoran arus adalah penting untuk meningkatkan prestasi fotovoltaik dalaman OSC. Dalam kajian ini, kepekatan larutan lapisan fotoaktif yang digabungkan titik kuantum karbon (CQDs) telah diubah untuk meningkatkan prestasi fotovoltaik di bawah pencahayaan 1-matahari dan LED putih dalaman. Lapisan fotoaktif terdiri daripada (6,6)-fenil-C61 butrik asid metal ester (PCBM) sebagai penerima dan poli (3-heksilthiofena) (P3HT) sebagai penderma. Lapisan pengangkut elektron ZnO dimendapkan pada substrat kaca bersalut oksida timah terdop fluorin (FTO) menggunakan teknik salutan putaran. Lapisan fotoaktif dengan kepekatan larutan yang berbeza disalut di atas lapisan ZnO. Untuk menghasilkan peranti, anod perak disejat secara terma. Adalah menarik untuk mendapati bahawa kepekatan larutan optimum yang diperoleh di bawah pencahayaan LED putih adalah lebih besar daripada di bawah pencahayaan 1-matahari. Kecekapan penukaran kuasa (PCE) maksimum 0.95% diperoleh di bawah pencahayaan 1-matahari untuk peranti dengan kepekatan larutan 36 mg/mL, manakala, di bawah pencahayaan LED putih, PCE tertinggi sebanyak 3.59% diperoleh untuk peranti dengan kepekatan larutan 48 mg/mL. Percanggahan itu adalah disebabkan oleh penyerapan cahaya yang lebih tinggi bagi lapisan fotoaktif yang lebih tebal dan kehilangan penggabungan semula cas yang kurang ketara di bawah keamatan cahaya yang lemah. Kajian ini menonjolkan kepentingan menggunakan strategi pengoptimuman yang berbeza untuk meningkatkan prestasi fotovoltaik OSC untuk aplikasi luaran dan dalaman.
Kata kunci: Arus bocor; ketebalan; penggabungan semula cas; penyerapan cahaya; titik kuantum karbon

INTRODUCTION

Organic solar cells (OSCs) are third generation photovoltaic devices. Due to their high mechanical flexibility, light weight, low production cost, reduced environmental effect, and ease of use, they have been recognized and taken into consideration as alternatives to inorganic solar cells as well as other nonrenewable energy sources that produce large amounts of carbon dioxide (Farooq et al. 2020; Lim et al. 2019; Majumder, Rai & Bose 2018; Taibi, Belghachi & Abid 2016; Yu et al. 2016; Yun & Sulaiman 2011). Further tunable optoelectronic properties, chemical customization, and large area fabrication are some other advantages which attract the researchers towards organic photovoltaic (Moustafa, Pallares & Marsal 2023). However, when compared to the previous two generations, the photovoltaic performance and stability of these third generation OSCs are rather poor under 1-sun illumination and outdoor situation (Farooq et al. 2020; Yan et al. 2020).

Due to the rise in popularity of different low power indoor electronic devices including the internet of things (IoT), sensors, and wearable technology in everyday human life, indoor photovoltaic (IPV) has attracted a lot of interest in recent years (Jahandar, Kim & Lim 2021; Khairulaman, Yap & Jumali 2021; Liu et al. 2020; Ma et al. 2020). These electronic devices are typically powered by conventional chemical batteries, which have a short lifespan and are bad for the environment. However, IPV is an energy harvesting technology that is dependable and has a longer lifespan and can be used in place of conventional chemical batteries (Li, Hou & Amaratunga 2021; Ma et al. 2020). Under white LED illumination, the power conversion efficiency (PCE) for indoor OSC has so far exceeded 31%, which is higher than that of silicon-based indoor solar cell (Alkhalayfeh et al. 2022; Ma et al. 2020). However, for an OSC to be effective in indoor application, a few crucial issues must be resolved. Due to the illuminating light intensity being substantially lower than the usual outdoor 1-sun illumination, the density of photogenerated charge carriers is much lower under indoor application. Thus, bimolecular charge recombination can be mitigated under low light illumination. However, it has been reported that the leakage current significantly affects the performance of indoor OSC (Liu et al. 2020; Ma et al. 2020; Park et al. 2018; Zhang, Duan & Ding 2020; Zhou et al. 2021). Therefore, to obtain indoor OSC with high PCE, minimizing leakage current and increasing exciton generation are essential.

Several studies have reported the photoactive layer solution concentration effects on the photovoltaic performance of OSCs based on poly (3-hexylthiophene) (P3HT): (6,6)-phenyl-C61-butyric acid methyl ester (PCBM). The light absorption of the device became higher when the photoactive layer was deposited from a more concentrated solution, resulting in higher photogenerated charge carriers (Ho et al. 2012). Meanwhile, it has also been reported that enhanced crystalline structure of P3HT donor domains was obtained from low concentration of photoactive layer solution, which contributed to the improved hole transport (Baek et al. 2009).

A recent study has reported that conditions for optimization of the photoactive layer of OSC under 1-sun illumination and white LED illumination are different (Khairulaman et al. 2022). It is well known that the light absorption of OSC improves with the increase of photoactive layer thickness, which leads to the enhancement of exciton generation (Moustafa, Pallares & Marsal 2023; Shaban et al. 2021; Shah et al. 2017; Sharma, Gupta & Singh Negi 2019; Ulum et al. 2019; Yu et al. 2016; Zang et al. 2018). However, under 1-sun illumination, the performance of OSC does not increase continuously with the increase of photoactive layer thickness. After some extent, the photovoltaic performance of OSC will drop drastically with the further increase of thickness due to inefficient charge transport and serious charge recombination loss (Ulum et al. 2019; Yu et al. 2016; Zang et al. 2018). In contrast, due to the low bimolecular charge recombination under low light illumination and small leakage current, the devices can perform even better with a thicker photoactive layer under white LED illumination (Liu et al. 2020; Shin et al. 2019). Therefore, different strategies of optimization of photoactive layer are needed to achieve a better photovoltaic performance under 1-sun and white LED illumination.

Although the photovoltaic performance of OSC has been improved significantly by introducing isopropanol (IPA) and carbon quantum dots (CQDs) into the photoactive layer under 1-sun illumination, the similar positive result was not achieved under white LED illumination (Wajidh et al. 2023). Therefore, it is expected that a better indoor photovoltaic performance could be obtained by optimizing the solution concentration of IPA/CQDs-incorporated photoactive layer. In this work, IPA/CQDs-incorporated P3HT:PCBM photoactive layers were prepared from different solution concentrations. Under 1-sun illumination, the optimum device was obtained with a solution concentration of 36 mg/mL, whereas the device with a higher solution concentration of 48 mg/mL exhibited the highest PCE under white LED illumination. The discrepancy is attributed to the enhanced light absorption and less significant bimolecular charge recombination loss.

MATERIALS AND METHODS

The inverted type OSCs were fabricated on glass substrates coated with fluorine tin oxide (FTO). On top of the FTO substrate, the ZnO thin film electron transport layer was deposited using a spin coating technique. Our previous work provides a detailed explanation of how ZnO thin film and CQDs were prepared (Issa et al. 2022). The P3HT donor and PCBM acceptor were used to prepare the photoactive layer solution in chlorobenzene solvent. Four different concentrations of photoactive layer solution, namely, 24, 36, 48, and 60 mg/mL were prepared and the weight ratio of P3HT to PCBM was kept at 1:1. The photoactive layer solutions were constantly stirred for 22 h at 850 rpm and at 60 °C. 2 wt% of CQDs and 40 vol% of IPA solvent were added to each photoactive layer solution. The photoactive layers were then spin coated on top of the ZnO layer. The

deposition was carried out in a glove box with low humidity of 15% at 1150 rpm for 60 s and room temperature of 25 °C. The samples were heated at 120 °C for 10 min after the deposition. Finally, at a vacuum condition of 5×10^{-5} mbar, the silver (Ag) was coated on top of the photoactive layer as anode by using a thermal evaporator. The active area of the devices was 0.07 cm^2.

A Keithley 2401 source measuring unit was used to measure the current-voltage (I-V) characteristics of devices under the illumination of a Newport 66902 AM1.5G solar simulator at 100 mW/cm^2 and a white LED at 1000 lx. The photovoltaic properties of the devices, including open circuit voltage (V_{oc}), short circuit current density (J_{sc}), fill factor (FF), and PCE were calculated from I-V curves. At a chopping frequency of 10 Hz, the incident photon to current efficiency (IPCE) of devices was determined with a Newport IPCE measurement system. Several characterizations were done on the photoactive layers in addition to device characterizations. The absorption spectra of photoactive layers in the wavelength range of 300 to 800 nm were measured using a Halo DB-20 UV-Vis spectrophotometer. In the meantime, a Nanosurf Easyscan2 atomic force microscope (AFM) was used to examine the morphology and surface roughness of the photoactive layers. Finally, to determine the thickness of photoactive layers, a Zeiss Merlin Compact field emission scanning electron microscope (FESEM) was used to capture the cross-sectional images of photoactive layers at a 3 kV accelerating voltage.

RESULTS AND DISCUSSION

The current density-voltage (J-V) characteristics of the devices prepared using four different photoactive layer solution concentrations under 1-sun illumination are shown in Figure 1. The photovoltaic parameters of the devices are listed in Table 1, and the data are averages across five devices. The J_{sc} initially increased with the increase of photoactive layer solution concentration and reached a lower value at a higher concentration of 60 mg/mL. The V_{oc} values also slightly varied with different solution concentrations of photoactive layer, but the variation is not significant. The other photovoltaic parameter FF decreased continuously with the increase of photoactive layer solution concentration. As a result, the device with photoactive layer solution concentration of 36 mg/mL achieved the highest PCE of 0.95% under 1-sun illumination.

A number of characterizations were carried out on the photoactive layer to identify the impact of photoactive layer solution concentration on the variation of different photovoltaic parameters of the devices. The UV-Vis absorption spectra of photoactive layers deposited using different solution concentrations are depicted in Figure 2(a). It is evident that when the photoactive layer solution concentration was raised, the light absorption increased gradually. The FESEM and AFM characterizations were carried out to identify the origin of enhanced light absorption. The cross-sectional FESEM images of the photoactive layers are shown in Figure 3, and Table 1 lists the matching photoactive layer thickness values. It is observed that the thickness of photoactive layer increased with the increase of photoactive layer solution concentration. It is generally accepted in a spin coating process that a thicker layer would be obtained from a more concentrated solution because of higher viscosity (Kang et al. 2019). As a result of increased photoactive layer thickness, more light could be absorbed by the photoactive layer (Moustafa, Pallares & Marsal 2023; Shaban et al. 2021; Shah et al. 2017; Sharma, Gupta & Singh Negi 2019; Ulum et al. 2019; Yu et al. 2016; Zang et al. 2018). Figure 4 shows the AFM surface images of the photoactive layers, and Table 1 lists the surface roughness values of each layer. Similar to the thickness, the surface roughness also increased with the increase of photoactive layer solution concentration. Other than larger thickness, the spin coating of a high concentration and viscosity solution also leads to layer with a roughened surface (Kang et al. 2019). As a result of internal reflection and scattering at the roughened surface, the amount of light absorbed increases too (Scholtz, Ladanyi & Mullerova 2014; Tadeson & Sabat 2019).

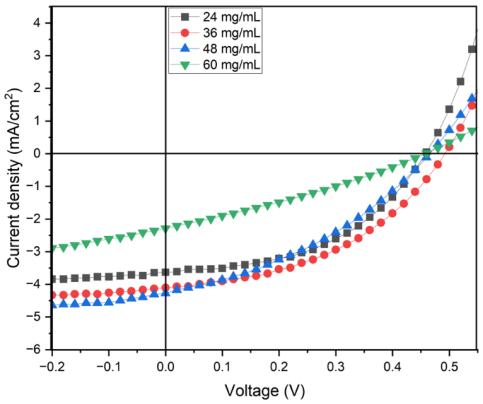

FIGURE 1. J-V curves of the devices under 1-sun illumination at 100 mWcm2

TABLE 1. Photovoltaic properties of the devices under 1-sun illumination (100 mWcm2) and 1000 lx white LED light (0.28 mWcm2)

	Light source	V_{oc} (V)	J_{sc} (μA/cm^2)	PCE (%)	FF (%)	R_s (Ωcm^2)	R_{sh} (Ωcm^2)	Roughness (nm)	Thickness (nm)
24 mg/mL	1-sun	0.45 ± 0.01	(3.65 ± 0.13) ×10^3	0.77 ± 0.07	47.0 ± 1.5	33.49	362.71	9.2 ± 0.42	167 ± 10
	White LED	0.15 ± 0.05	37.2 ± 2.0	0.66 ± 0.30	32.9 ± 4.9				
36 mg/mL	1-sun	0.48 ± 0.00	(4.17 ± 0.18) ×10^3	0.95 ± 0.07	47.4 ± 1.6	40.55	665.27	10.3 ± 0.32	216 ± 9
	White LED	0.30 ± 0.01	56.7 ± 2.8	2.37 ± 0.27	39.0 ± 3.0				
48 mg/mL	1-sun	0.46 ± 0.03	(4.28 ± 0.19) ×10^3	0.79 ± 0.06	40.2 ± 1.0	51.47	443.19	15.8 ± 0.28	368 ± 7
	White LED	0.33 ± 0.03	72.7 ± 2.2	3.59 ± 0.26	42.3 ± 3.0				
60 mg/mL	1-sun	0.43 ± 0.01	(2.52 ± 0.23) ×10^3	0.33 ± 0.04	30.4 ± 0.7	126.55	265.99	19.6 ± 0.49	461 ± 14
	White LED	0.29 ± 0.03	66.6 ± 6.4	2.69 ± 0.28	39.0 ± 3.8				

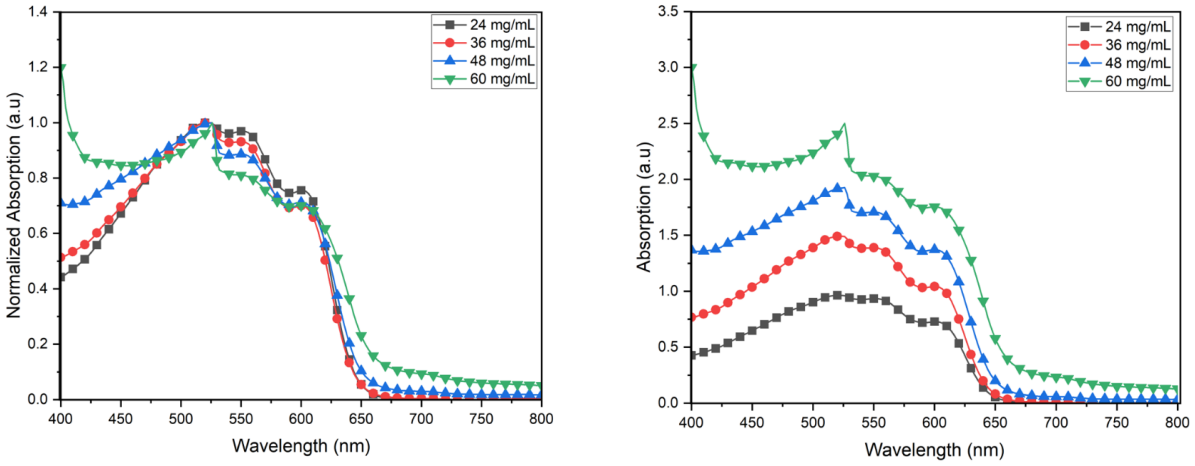

(a) (b)

FIGURE 2. (a) UV–Vis absorption spectra and (b) normalized UV–Vis absorption spectra of the photoactive layers

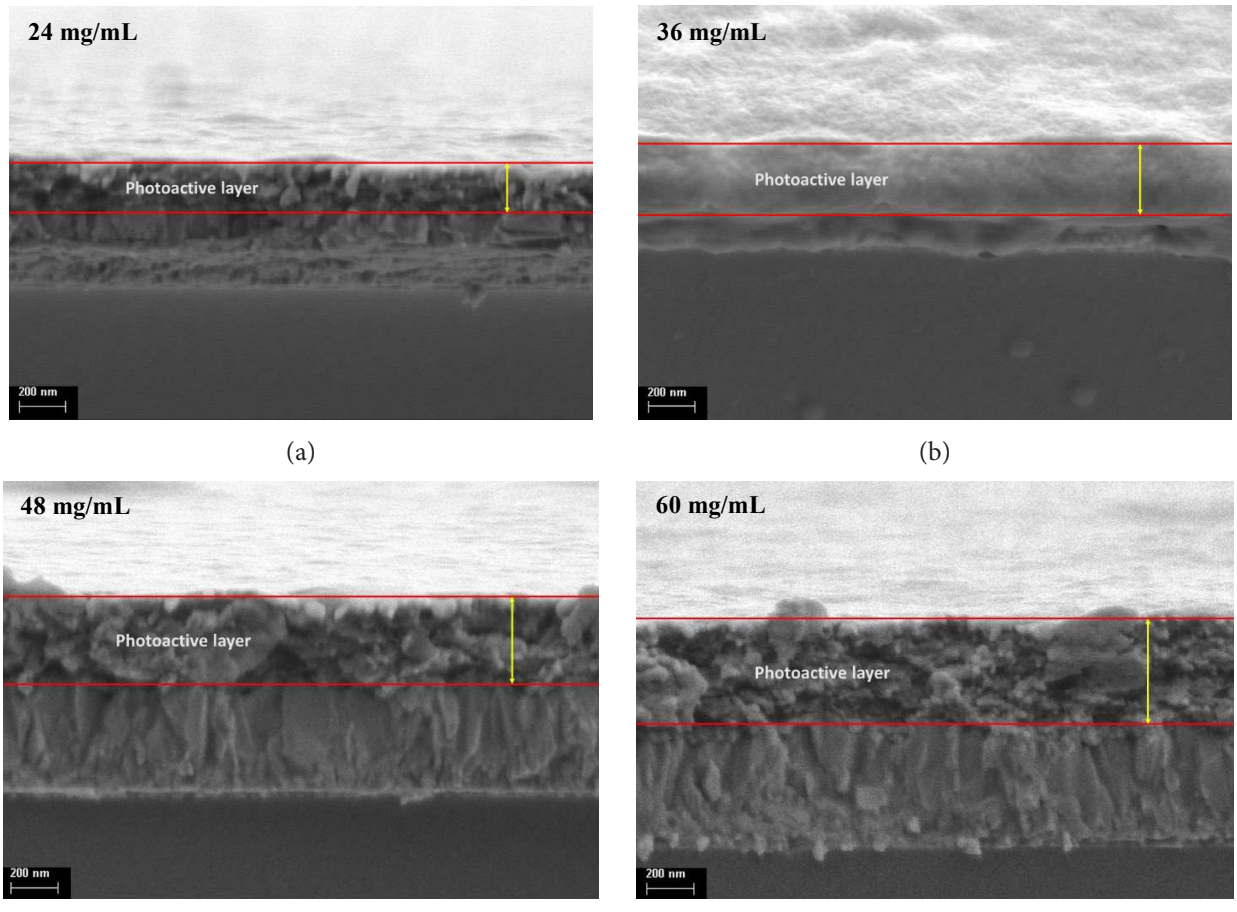

(a) (b)

(c) (d)

FIGURE 3. FESEM cross section images of photoactive layers prepared using solution concentration of (a) 24 mg/mL, (b) 36 mg/mL, (c) 48 mg/mL, and (d) 60 mg/mL

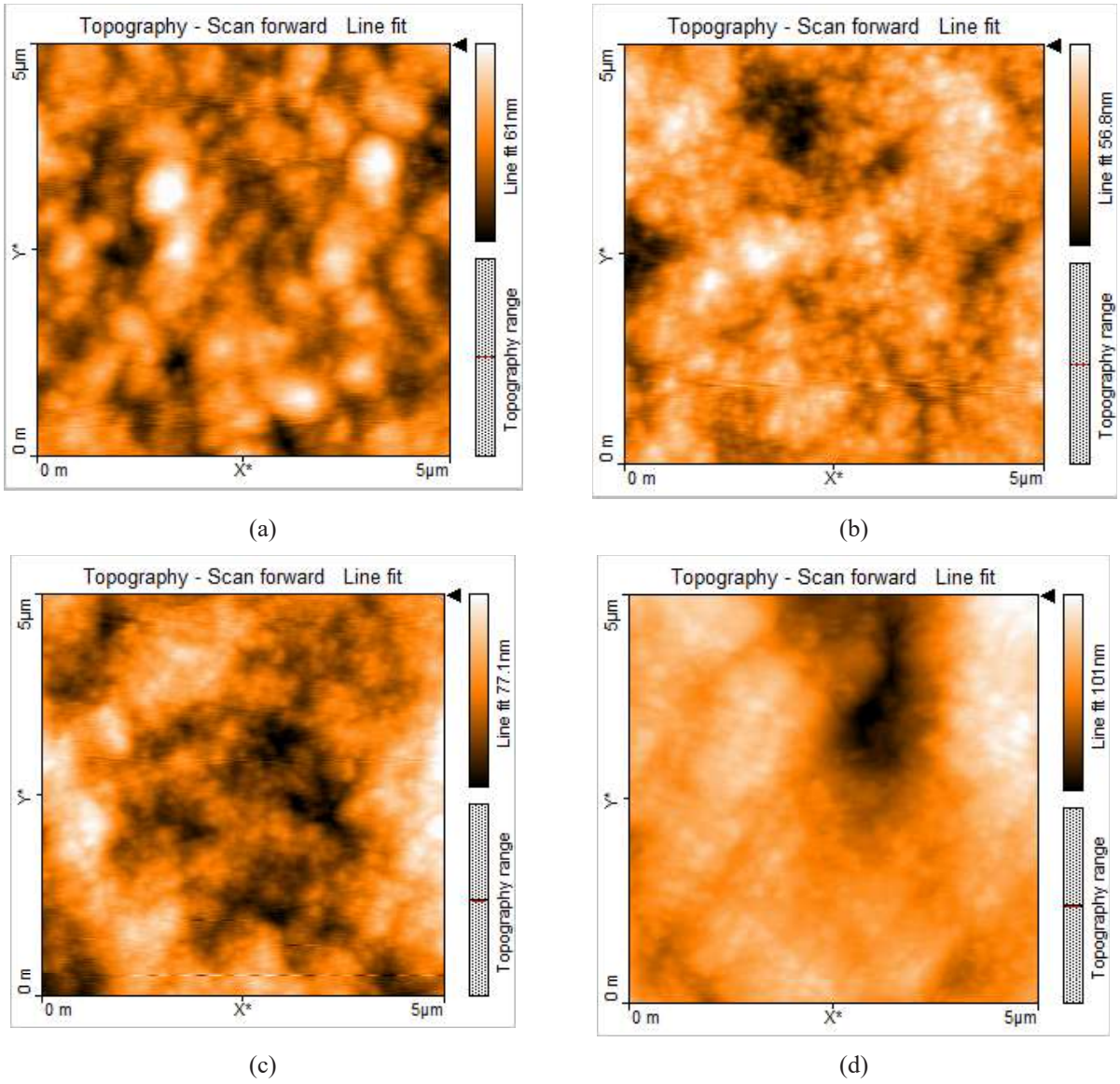

FIGURE 4. AFM topography images of photoactive layers prepared using solution concentration of (a) 24 mg/mL, (b) 36 mg/mL, (c) 48 mg/mL, and (d) 60 mg/mL. Scan size is 5 µm × 5 µm

The J_{sc} does not follow the trend of light absorption completely. The J_{sc} dropped drastically at the highest solution concentration of 60 mg/mL although the highest light absorption was achieved at that concentration. It is agreed that higher light absorption produces a larger number of excitons and free charge carriers. However, the free charge carriers must travel relatively longer pathway in a thicker photoactive layer to reach the electrodes, and there is a higher possibility of bimolecular charge recombination loss which leads to reduction in J_{sc} (Moustafa, Pallares & Marsal 2023; Sharma, Gupta & Singh Negi 2019; Ulum et al. 2019; Yu et al. 2016). This behavior is supported by the series resistance (R_s) which increased with the increase of photoactive layer thickness. In addition, the increase of surface roughness also contributes to the increase of interfacial contact resistance between photoactive layer and the anode as reflected by larger value of R_s (Hazar Apaydin et al. 2013). Figure 5 shows the I-V curves of the devices under dark condition. The forward bias dark current was found to be decreased with increasing photoactive layer solution concentration, which is consistent with the trend of R_s.

Figure 2(b) shows the normalized UV-Vis spectra of photoactive layers prepared using different solution concentrations. It can be noticeable that the shoulder peak at ~ 550 nm of photoactive layer prepared with low solution concentration is more obvious than that of high solution concentration sample. The intensity of shoulder peak at ~

550 nm increased with the decrease of photoactive layer solution concentration. This observation implies that an improved P3HT chain ordering and better hole mobility in the P3HT region were obtained at low solution concentration (Baek et al. 2009; Xu et al. 2019). This result agrees well with previous research that slower evaporation rate of a less concentrated solution leads to stronger P3HT interchain interactions (Baek et al. 2009). The decrease of P3HT chain ordering and hence hole mobility with increasing solution concentration also contribute to the reduction of J_{sc}, particularly at the highest solution concentration of 60 mg/mL (Hazar Apaydin et al. 2013; Zang et al. 2018).

The FF is another crucial photovoltaic parameter that has an impact on the PCE of device. A high value of FF can be achieved with a low R_s and a high shunt resistance (R_{sh}). The drastic reduction of FF at solution concentrations of 48 and 60 mg/mL can be ascribed to decrease of R_{sh} and increase of R_s, as indicated by the declining of I-V curve squareness (Sharma, Gupta & Singh Negi 2019). Decrease of R_{sh} is an indication of increased charge recombination and larger leakage current (Moustafa, Pallares & Marsal 2023; Sharma, Gupta & Singh Negi 2019; Yu et al. 2016; Zang et al. 2018). It is believed that higher charge recombination in a thicker photoactive layer (48 and 60 mg/mL) and larger leakage current in thinner photoactive layer (24 mg/mL) lead to a smaller value of Rsh. This result is further evidenced by the dark I-V curve in Figure 5. The leakage current of the device as indicated by the reverse biased current decreased with the increase of photoactive layer solution concentration. It has been reported previously that the device with a thinner active layer suffers higher leakage current due to the higher number of pinholes which act as path for current leakage (Shah et al. 2017; Shin et al. 2019).

Figure 6 shows the IPCE spectra of devices. The IPCE indicates the efficiency of conversion of incident photon into the charge carriers at external circuit. The IPCE trend is correlated well with Jsc behavior. All devices exhibited a broad IPCE spectrum in the range of 325 to 650 nm. The J_{sc} values obtained from IPCE measurements were 3.57, 4.20, 4.26, and 2.26 mA/cm2 for the devices with photoactive layer solution concentrations of 24, 36, 48, and 60 mg/mL, respectively. These values agree closely with J_{sc} values extracted from the J-V curve.

V_{oc} is another photovoltaic parameter that determines the PCE of device. There is a slight variation in V_{oc} with different photoactive layer solution concentrations, in which the lowest value of V_{oc} was recorded at the highest concentration of 60 mg/mL. As reported previously, the V_{oc} is dependent on the separation between quasi fermi levels in the photoactive layer (Sharma, Gupta & Singh Negi 2019). The quasi fermi levels in an illuminated OSC show the energy differential between the holes in the valence band and the electrons in the conduction band. This distinction determines the V_{oc}. At high solution concentration, the charge recombination loss in thick photoactive layer will be higher due to charge carriers have to travel longer path to reach their respective electrodes. The quantity of photo-generated carriers that are still free and available for conduction decreases with increase of charge recombination. As a result, separation between the quasi fermi levels of the electrons and holes decreases, resulting in a reduction in overall V_{oc}.

Figure 7 shows the J-V characteristics of the devices under white LED illumination. The photovoltaic parameters of the devices extracted from the corresponding J-V curves are listed in Table 1. The PCEs of the devices with photoactive layer solution concentrations of 24, 36, 48, and 60 mg/mL were 0.66% (Pmax = 1.86 μW cm2), 2.37% (Pmax = 6.62 μW cm2), 3.59% (Pmax = 10.07 μW cm2), and 2.69% (Pmax = 8.39 μW cm2), respectively. It has been reported that electric power in the range of 1 to 100 μW is usually consumed by low-power electronic devices under idle or standby state (Alkhalayfeh et al. 2022; Ma et al. 2020; Shin et al. 2019). Therefore, these devices are acceptable for indoor applications. Under white LED illumination, the PCEs of the devices with solution concentrations of 36, 48, and 60 mg/mL were improved by approximately ~2-fold, ~5-fold and ~8-fold, respectively, compared to that under 1-sun illumination. In contrast, the device with the lowest solution concentration of 24 mg/mL performed much poorer under white LED illumination.

Since the photogenerated current density is relatively high under 1-sun illumination, the effect of leakage current usually can be neglected. However, under white LED illumination with very weak light intensity, the leakage current has a significant impact on the photovoltaic performance, especially the Voc and FF (Ma et al. 2020; Zhou et al. 2021). It can be observed in Figure 5 that the device with solution concentration of 24 mg/mL experienced the largest leakage current, resulting in much reduced values of V_{oc} and FF. In addition to leakage current factor, the reduced light absorption and exciton production due to relatively thin photoactive layer also contribute to poor photovoltaic performance. Unlike 1-sun illumination, the highest PCE of 3.59% was obtained for the device with solution concentration of 48 mg/mL under white LED illumination, owning to the smaller charge recombination loss at lower charge concentration. The increment of PCE is mainly attributed to the increased FF as a result of lower leakage current and charge recombination (Ma et al. 2020; Zhou et al. 2021). It indicates that the devices with thicker photoactive layer showed better performance under indoor white LED illumination in contrast to their performance under 1-sun illumination due to higher light absorption and less significant bimolecular charge recombination loss under weak light intensity. It is interesting to find that the device with solution concentration of 60 mg/mL did not exhibit a drastic PCE drop under white LED illumination. This result suggests that the indoor photovoltaic performance is less sensitive to the photoactive layer thickness. Different solution concentration optimization of photoactive layer is needed under 1-sun and white LED illumination.

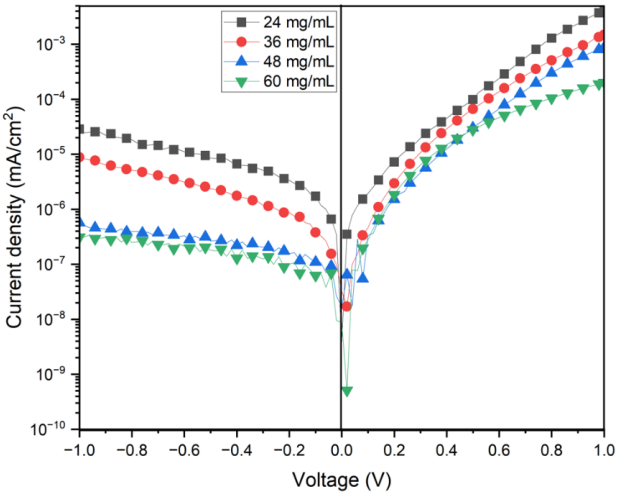

FIGURE 5. I-V curves of the devices under dark condition

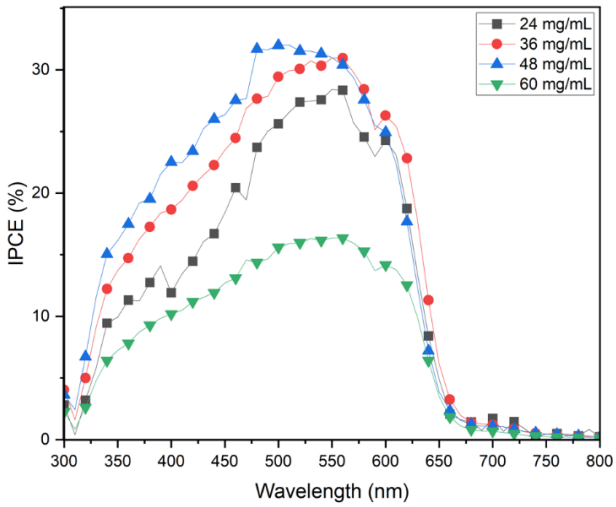

FIGURE 6. IPCE spectra of the devices

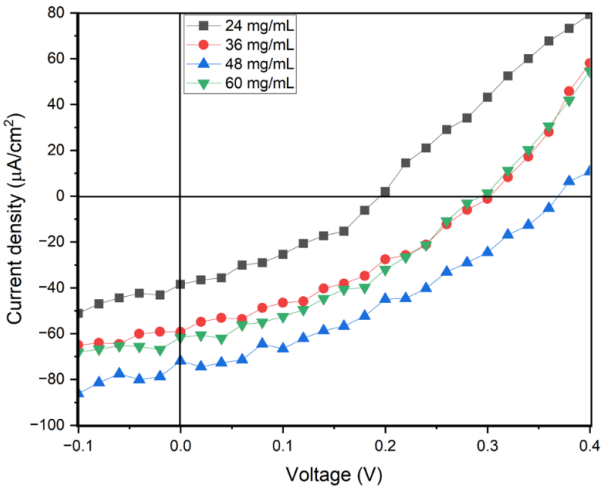

FIGURE 7. J-V curves of the devices under white LED illumination at 1000 lx

CONCLUSION

In conclusion, the solution concentration of photoactive layer demonstrated a different impact on the photovoltaic performance of devices under 1-sun and indoor white LED illumination. The optimum solution concentrations were 36 and 48 mg/mL for the devices tested under 1-sun and white LED illumination, respectively. The discrepancy is attributed to the higher light absorption of thicker photoactive layer and less significant bimolecular charge recombination loss under weak light intensity. The devices under white LED illumination also showed a wider tolerance of photoactive layer thickness except for the lowest solution concentration of 24 mg/mL, in which the larger leakage current played a dominant role. More importantly, different optimization strategies in terms of the photoactive layer solution concentration would be required to optimize the device performance for outdoor and indoor applications.

ACKNOWLEDGEMENTS

The research was funded by the Ministry of Higher Education (MOHE), Malaysia through the Fundamental Research Grant Scheme (FRGS) under the grant number (FRGS/1/2020/STG07/UKM/02/4). The analytical services were provided by i-CRIM Centralized Lab, Universiti Kebangsaan Malaysia.

REFERENCES

Alkhalayfeh, M.A., Abdul Aziz, A., Pakhuruddin, M.Z., Katubi, K.M.M. & Ahmadi, N. 2022. Recent development of indoor organic photovoltaics. *Physica Status Solidi (A) Applications and Materials Science* 219: 2100639.

Baek, W.H., Yang, H., Yoon, T.S., Kang, C.J., Lee, H.H. & Kim, Y.S. 2009. Effect of P3HT:PCBM concentration in solvent on performances of organic solar cells. *Solar Energy Materials and Solar Cells* 93(8): 1263-1267.

Farooq, W., Khan, A.D., Khan, A.D. & Noman, M. 2020. Enhancing the power conversion efficiency of organic solar cells. *Optik* 208: 164093.

Hazar Apaydin, D., Esra Yildiz, D., Cirpan, A. & Toppare, L. 2013. Optimizing the organic solar cell efficiency: Role of the active layer thickness. *Solar Energy Materials and Solar Cells* 113: 100-105.

Ho, C.S., Huang, E.L., Hsu, W.C., Lee, C.S., Lai, Y.N., Yao, E.P. & Wang, C.W. 2012. Thermal effect on polymer solar cells with active layer concentrations of 3-5 wt%. *Synthetic Metals* 162(13-14): 1164-1168.

Issa, N.A., Yap, C.C., Tan, S.T., Hong, K.J., Lau, K.S., Khairulaman, F.L., Chia, C.H., Jumali, M.H.H. & Chong, K-K. 2022. Photovoltaic performance improvement of organic solar cell with ZnO nanorod arrays as electron transport layer using carbon quantum dots-incorporated photoactive layer. *Optical Materials* 132: 112876.

Jahandar, M., Kim, S. & Lim, D.C. 2021. Indoor organic photovoltaics for self-sustaining IoT devices: Progress, challenges and practicalization. *ChemSusChem* 14: 3449-3474.

Kang, M.H., Heo, D.K., Kim, D.H., Lee, M., Ryu, K., Kim, Y.H. & Yun, C. 2019. Fabrication of spray-coated semitransparent organic solar cells. *IEEE Journal of the Electron Devices Society* 7: 1129-1132.

Khairulaman, F.L., Yap, C.C. & Jumali, M.H.H. 2021. Improved performance of inverted type organic solar cell using copper iodide-doped P3HT:PCBM as active layer for low light application. *Materials Letters* 283: 128827.

Khairulaman, F.L., Yap, C.C., Jumali, M.H.H. & Issa, N.A. 2022. Optimization of CuI-doped P3HT:PCBM layers in inverted-type organic solar cells for indoor light applications. *Sains Malaysiana* 51(12): 4059-4069.

Li, B., Hou, B. & Amaratunga, G.A.J. 2021. Indoor photovoltaics, The Next Big Trend in solution-processed solar cells. *InfoMat* 3: 445-459.

Lim, E. L., Yap, C. C., Jumali, M. H. H. & Khairulaman, F. L. 2019. Solution-dispersed copper iodide anode buffer layer gives P3HT:PCBM-based organic solar cells an efficiency boost. *Journal of Materials Science: Materials in Electronics* 30(3): 2726–2731.

Liu, J., Cui, Y., Zu, Y., An, C., Xu, B., Yao, H., Zhang, S. & Hou, J. 2020. Organic photovoltaic cells for low light applications offering new scope and orientation. *Organic Electronics* 85: 105798.

Ma, L-K., Chen, Y., Chow, P.C.Y., Zhang, G., Huang, J., Ma, C., Zhang, J., Yin, H., Cheung, A.M.H., Wong, K.S., So, S.K. & Yan, H. 2020. High-efficiency indoor organic photovoltaics with a band-aligned interlayer. *Joule* 4(7): 1486-1500.

Majumder, C., Rai, A. & Bose, C. 2018. Performance optimization of bulk heterojunction organic solar cell. *Optik* 157: 924-929.

Moustafa, E., Pallares, J. & Marsal, L.F. 2023. Investigating the role of PM6:Y7 layer thickness on optimizing non-fullerene organic solar cells performance through impedance spectroscopy analysis. *IEEE Journal of the Electron Devices Society* 11: 642-649.

Park, S.Y., Li, Y., Kim, J., Lee, T.H., Walker, B., Woo, H.Y. & Kim, J.Y. 2018. Alkoxybenzothiadiazole-based fullerene and nonfullerene polymer solar cells with high shunt resistance for indoor photovoltaic applications. *ACS Applied Materials and Interfaces* 10(4): 3885-3894.

Scholtz, L., Ladanyi, L. & Mullerova, J. 2014. Influence of surface roughness on optical characteristics of multilayer solar cells. *Advances in Electrical and Electronic Engineering* 12(6): 631-638.

Shaban, M., Benghanem, M., Almohammedi, A. & Rabia, M. 2021. Optimization of the active layer P3HT:PCBM for organic solar cell. *Coatings* 11(7): 863.

Shah, S.K., Khan, J., Ullah, I. & Khan, Y. 2017. Optimization of active-layer thickness, top electrode and annealing temperature for polymeric solar cells. *AIMS Materials Science* 4(3): 789-799.

Sharma, N., Gupta, S.K. & Singh Negi, C.M. 2019. Influence of active layer thickness on photovoltaic performance of PTB7:PC70BM bulk heterojunction solar cell. Superlattices and Microstructures 135: 106278.

Shin, S.C., Koh, C.W., Vincent, P., Goo, J.S., Bae, J.H., Lee, J.J., Shin, C., Kim, H., Woo, H.Y. & Shim, J.W. 2019. Ultra-thick semi-crystalline photoactive donor polymer for efficient indoor organic photovoltaics. Nano Energy 58: 466-475.

Tadeson, G. & Sabat, R.G. 2019. Enhancement of the power conversion efficiency of organic solar cells by surface patterning of azobenzene thin films. ACS Omega 4(26): 21862-21872.

Taibi, I., Belghachi, A. & Abid, H. 2016. Effect of trapping and temperature on the performance of P3HT: PCBM organic solar cells. Optik 127(20): 8592-8599.

Ulum, M.S., Sesa, E., Kasman & Belcher, W. 2019. The effect of active layer thickness on P3HT:PCBM nanoparticulate organic photovoltaic device performance. Journal of Physics: Conference Series 1242(1): 012025.

Wajidh, M.N., Yap, C.C., Issa, N.A., Lau, K.S., Tan, S.T., Jumali, M.H.H., Mustapha, M. & Chia, C.H. 2023. Photovoltaic performance improvement of inverted type organic solar cell by co-introducing isopropanol and carbon quantum dots in photoactive layer. Journal of Materials Science: Materials in Electronics 34: 1075.

Xu, B., Sai-Anand, G., Unni, G.E., Jeong, H.M., Kim, J.S., Kim, S.W., Kwon, J.B., Bae, J.H. & Kang, S.W. 2019. Pyridine-based additive optimized P3HT:PC61BM nanomorphology for improved performance and stability in polymer solar cells. Applied Surface Science 484: 825-834.

Yan, N., Zhao, C., You, S., Zhang, Y. & Li, W. 2020. Recent progress of thin-film photovoltaics for indoor application. Chinese Chemical Letters 31(3): 643-653.

Yu, H., Li, Y., Dong, Y. & Huang, X. 2016. Fabrication and optimization of polymer solar cells based on P3HT:PC70BM system. International Journal of Photoenergy 2016: 702-709.

Yun, T.W. & Sulaiman, K. 2011. Fabrication and morphological characterization of hybrid polymeric solar cells based on P3HT and inorganic nanocrystal blends. Sains Malaysiana 40(1): 43-47.

Zang, Y., Xin, Q., Zhao, J. & Lin, J. 2018. Effect of active layer thickness on the performance of polymer solar cells based on a highly efficient donor material of PTB7-Th. Journal of Physical Chemistry C 122(29): 16532-16539.

Zhang, Y., Duan, C. & Ding, L. 2020. Indoor organic photovoltaics. Science Bulletin 65: 2040-2042.

Zhou, X., Wu, H., Lin, B., Naveed, H.B., Xin, J., Bi, Z., Zhou, K., Ma, Y., Tang, Z., Zhao, C., Zheng, Q., Ma, Z. & Ma, W. 2021. Different morphology dependence for efficient indoor organic photovoltaics: The role of the leakage current and recombination losses. ACS Applied Materials and Interfaces 13(37): 44604-44614.

*Corresponding author; email: ccyap@ukm.edu.my